ACS APPLIED MATERIALS & INTERFACES

Research Article

www.acsami.org

Facile Synthesis of Size Controllable Dendritic Mesoporous Silica Nanoparticles

Ye-Jun Yu,[†] Jun-Ling Xing,[†] Jun-Ling Pang,[†] Shu-Hua Jiang,[†] Koon-Fung Lam,[‡] Tai-Qun Yang,[†] Qing-Song Xue,[†] Kun Zhang,*[,†] and Peng Wu[†]

[†]Shanghai Key Laboratory of Green Chemistry and Chemical Processes, Department of Chemistry, East China Normal University, No. 3663 Zhongshan North Road, 200062 Shanghai, China

[‡]Department of Chemical Engineering, University College London, Torrington Place, London, United Kingdom

Supporting Information

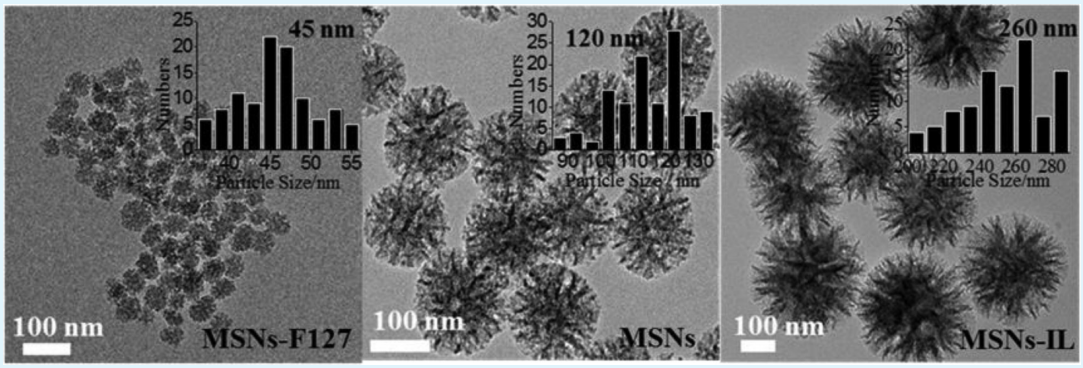

ABSTRACT: The synthesis of highly uniform mesoporous silica nanospheres (MSNs) with dendritic pore channels, particularly ones with particle sizes below 200 nm, is extremely difficult and remains a grand challenge. By a combined synthetic strategy using imidazolium ionic liquids (ILs) with different alkyl lengths as cosurfactants and Pluronic F127 nonionic surfactants as inhibitors of particle growth, the preparation of dendritic MSNs with controlled diameter between 40 and 300 nm was successfully realized. An investigation of dendritic MSNs using scanning electron microscopy (SEM), transmission electron microscopy (TEM), and nitrogen physisorption revealed that the synthesis of dendritic MSNs at larger size (100−300 nm) strongly depends on the alkyl lengths of cationic imidazolium ILs; while the average size of dendritic MSNs can be controlled within the range of 40−100 nm by varying the amount of Pluronic F127. The Au@MSNs can be used as a catalyst for the reduction of 4-nitrophenol by $NaBH_4$ into 4-aminophenol and exhibit excellent catalytic performance. The present discovery of the extended synthesis conditions offers reproducible, facile, and large-scale synthesis of the monodisperse spherical MSNs with precise size control and, thus, has vast prospects for future applications of ultrafine mesostructured nanoparticle materials in catalysis and biomedicine.

KEYWORDS: *colloidal mesoporous silica nanoparticles, alkyl imidazolium ionic liquids, size control, growth inhibitor*

INTRODUCTION

Monodisperse mesoporous silica nanoparticles with controllable particle size, also called colloidal mesoporous silica nanoparticles, attract much research interests in recent years because of their potential applications in chromatography, cosmetics, catalysis, and adsorption, as mesoporous nanoparticles provide greater pore accessibility and fast molecular diffusion.[1,2] In particular, the dendritic mesoporous silica nanospheres with a radiation-aligned mesopores in size below 200 nm were found to be applicable to biomedical and pharmaceutical fields such as drug, gene, protein, imaging agent delivery, and biosensors.[3−10] To date, great efforts have been put on the development of recipes for the synthesis of mesoporous silica nanoparticles. Most pathways for the production of mesoporous silica nanospheres (MSNs) rely on the sol−gel soft-templating strategy, which was reported by the groups of Cai,[11] Mann,[12] Ostafin,[13] and Lin.[14] Despite the control achieved over the particle size, colloidal stability, and morphology of ordered mesoporous nanoparticles, major drawbacks of the soft-templating methods remain at, namely, low silica concentrations used, one-fold mesostructure (generally worm-like pore), and low yields.[15−20] Recently, the synthesis strategy reported by Polshettiwar provides a benchmark for producing well-defined porous silica nanospheres with fibrous pore morphology, so-called dendritic MSNs (named KCC-1).[21] However, these structures are either too large (>200 nm) for application in life sciences or too complex to be produced at a large scale.[22−26] Thus, a reliable large-scale production of MSNs with tunable porosity and

Received: October 2, 2014
Accepted: December 2, 2014
Published: December 2, 2014

particle size, particularly <200 nm, is highly desirable. Notably, by mimicking the self-assembling interaction between cationic surfactants and inorganic silicates, we successfully synthesized MSNs with tunable mesostructures and size less than 150 nm at kilogram scale and found that tosylate (Tos^-) counteranions of surfactant favored dendritic morphologies at ultra low triethanolamine ($TEAH_3$) concentrations.[27] These materials exhibited the highly hydrothermal stability: the morphology and mesostructure were maintained after high-temperature steam post-treatment at 700 °C for 6 h.[27] However, the size-controllable synthesis of dendritic MSNs by this methodology is not realized due to the intrinsic nature of this method, i.e. the nucleation and growth of dendritic MSNs is not sensitive to the modulation of reaction parameters such as temperature and volume ratio of water to ethanol. To our best knowledge, the size-controlled synthesis of dendritic MSNs below 200 nm is not precedent for success. Thus, the development of new methods to synthesize dendritic MSNs with tunable sizes is a pressing need.

In this study, we demonstrate a simple method for size-controlled synthesis of uniform dendritic MSNs with the introduction of ILs and F127 in the synthesis process. The dendritic MSNs, which are composed of radiation-aligned mesopores, have nearly monodispersed sizes/diameters that are tunable in the range of 40−300 nm by varying the concentration and alkyl chain length of the ILs and the amount of F127. The mechanism leading to the size tunability is discussed.

EXPERIMENTAL SECTION

Materials. Cetyltrimethylammonium tosylate (CTATos) was purchased from MERCK (The use of CTATos as surfactant templates for the synthesis of mesoporous materials has several advantages: low cost because of the use of ultralow concentration surfactant, readily handling without any foams during the product collection, and scale-up production of mesoporous silica with different topology structures).[29,30] Triethanolamine ($TEAH_3$), tetraethylorthosilicate (TEOS), chloroauric acidtetrahydrate ($HAuCl_4{\cdot}4H_2O$), 4-nitrophenol (4-NP), and sodium borohydride ($NaBH_4$) were purchased from Sinopharm Chemical Reagent Co., Ltd. All ionic liquids were purchased from Sinopharm Chemical Reagent Co., Ltd. Poly(ethylene oxide)-*b*-poly(propylene oxide)-*b*-poly(ethylene oxide) triblock copolymer F127 (EO106PO70EO106, MW = 12 600) and (3-aminopropyl) trimethoxysilane (APTMS) were purchased from Aldrich. All chemicals were used as received without any further purification. Deionized water was used in all experiments.

Characterization. The SEM and TEM images were taken using Hitachi S-4800 microscope and JEOL-JEM-2100 microscope, respectively. Nitrogen adsorption−desorption isotherms were obtained at 77 K on a BEL SORP after activating the sample under vacuum at 573 K for 6 h, and *it is worth noting that the powder of dendritic MSNs calcined at 550 °C for 6 h was pelleted at 10 MPa before the nitrogen adsorption measurement to avoid the contribution of interparticles void into the total volume and surface area.* FT-IR spectra of as-made MSNs were recorded by Nicolet Fourier transform infrared spectrometer (NEXUS 670) using the KBr technique. Thermogravimetric analysis (TG) was performed on a Mettler TGA/SDTA 851e instrument with a heating rate of 10 °C/min under an air flow. Ultraviolet visible (UV−vis) spectroscopy was conducted with a UV2500 UV−vis spectrophotometer.

Synthesis of Mesoporous Silica Nanoparticles in the Presence of Ionic Liquids and F127. Particle sizes of dendritic MSNs were controlled by adjusting the concentration and alkyl length of imidazolium ionic liquid and the amounts of F127 in the TEOS-CTATos-$TEAH_3$-water synthesis solution.[27] A typical synthesis of MSNs was performed as follows: 1.92 g of CTATos, 0.21 g of $TEAH_3$, 0.02 g of 1-butyl-3-methylimidazolium trifluoro-methanesulfonate ([BMIM] OTF), and 100 mL of deionized water were mixed and then stirred at 80 °C for 1 h. After that, 14.58 g of TEOS was quickly added into the solution. The final mixture was stirred for 2 h. The mother liquid molar ratio is $1.0SiO_2$:0.06CTATos:$0.026TEAH_3$:$80H_2O$:0.00095[BMIM] OTF. The synthesized MSNs were centrifuged, washed, and dried in the oven at 100 °C overnight. The products were denoted as MSNs-C*n*-*X*, where *X* represents molar ratio of IL or F127 to TEOS and *n* represents the carbon atom numbers in the alkyl chain of methylimidazolium ILs.

Synthesis of Mesoporous Silica Nanoparticles Loaded with Gold Nanoparticles (Au@MSNs). The Au@MSNs catalysts were fabricated by amino-functionalizing the MSNs-C4 and then grafting the gold nanoparticles. In a typical process, 40 mL of anhydrous ethanol, 1 g of the calcined MSNs-C4, and 1.5 g of APTMS were introduced into the round-bottom flask and the mixture was refluxed at 80 °C for 12 h. The solution was filtered, and the solid was washed with ethanol and dried overnight at 80 °C. After that, 0.125 g of solid, 2.5 mL aqueous solution of $HAuCl_4$ (4.85×10^{-3} mol/L), and 10 mL H_2O were mixed and stirred at room temperature for 12 h, and then 0.03 g of $NaBH_4$ was added into the suspension. The obtained solid material was filtered and washed repeatedly with deionized water and ethanol and dried overnight at 80 °C.

Reduction of 4-Nitrophenol. The catalytic properties of Au@MSNs were investigated via the reduction of 4-nitrophenol (4-NP) to 4-aminophenol (4-AP) as a model reaction with $NaBH_4$ as the reductant. Aqueous solutions of 4-NP (0.2 mL, 2.5 mM) and $NaBH_4$ (0.4 mL, 250 mM) were added into a quartz cuvette under stirring. Subsequently, 0.1 mL of aqueous solution of Au@MSNs (5 mg/mL) was added. As the reaction progressed the bright yellow solution gradually faded.

RESULTS AND DISCUSSION

The dendritic mesoporous silica nanoparticles were synthesized following our previously reported process with cetyltrimethylammonium (CTA^+) as the templating surfactant and small organic amines as the mineralizing agent. In the previous study, we found that the kilogram scale synthesis of pure nanophases of monodisperse MSNs smaller than 130 nm with stellate, raspberry, or worm-like morphologies strongly depended on the nature and the concentration (pH value) of small organic amines together with an appropriate choice of the cationic surfactant counterions.[27] In this study, we found that dendritic MSNs were synthesized only at ultralow concentration of small organic amines with strong hydrogen-bond interaction, such as triethanolamine ($TEAH_3$) in the presence of surfactant counteranion, namely, tosylate (Tos^-). The size of dendritic MSNs was not sensitive to the variation of reaction temperature and time, which is in contrast to the discovery of Stöber method for the synthesis of monodisperse silica nanoparticles.[31] Stöber's approach is to obtain smaller sized silica nanoparticles by adjusting the surface tension of the synthesis solution, i.e., increasing the quotient of water or the volume ratio of alcohol/water.[32] However, this way is not suitable for the synthesis of dendritic MSNs because of the formation of undesired mesophases when these reaction parameters are changed. Our preliminary results show that the reaction kinetic on the synthesis of dendritic MSNs by liquid crystal templating self-assemblybetween surfactants and silicates is actuallydifferent from that of Stöber silica beads.[27]

In order to successfully synthesize the dendritic MSNs with uniform and controllable particle size, the size control agent needs to fulfill the following two basic conditions: it cannot affect the self-assembly mechanism between surfactant and silicates nor change the synthetic phase including the pH of reaction medium. Inspired by the size-controllable synthesis of other functional nanomaterials such as metal and metal oxide nanoparticles,[33−36] carbon nanoparticles,[37−40] mesoporous

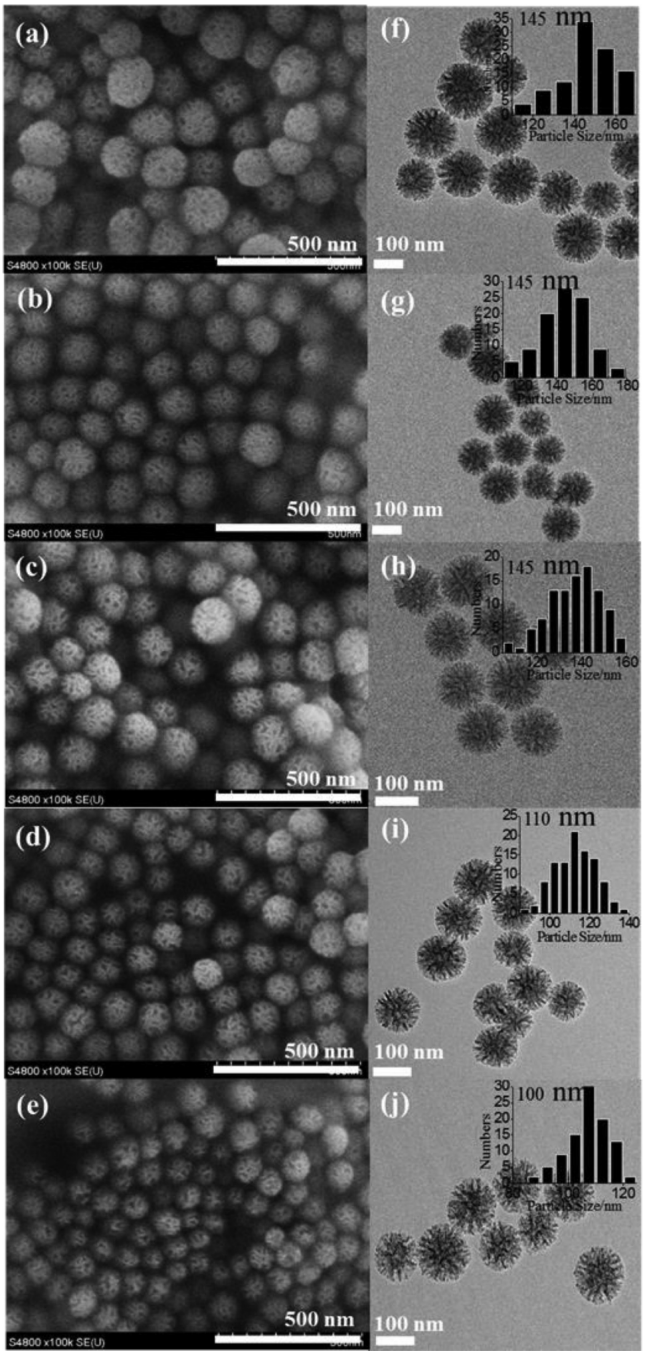

Figure 1. SEM and TEM images of dendritic MSNs synthesized with different alkyl chain length in methylimidazolium bromide: n = (a and f) 4, (b and g) 8, (c and h) 10, (d and i) 12, and (e and j) 16.

silica nanoparticls,[18] nanozeolites,[41,42] metal–organic frameworks (MOF),[43] and other inorganic–organic hybrids,[44] we proved that ionic liquid (ILs) and nonionic block copolymer can act as good size-controllable agents for the synthesis of dendritic MSNs with a systematic investigation ofthe type and amount of methylimidazolium ILs and concentration of Pluronic F127 on the particle size of dendritic MSNs.

Effect of the Alkyl Chain Length of Imidazolium Bromide ([CnMIM]Br). The size, morphology, and structure of the dendritic MSNs samples synthesized using different alkyl chain length of methylimidazolium bromide as cosurfactants under optimum conditions were investigated using electron microscopy. As shown in the scanning electron microscopy (SEM) images of Figure 1, all MSNs are spherical in shape with a uniform particle size (100–150 nm) (Figure 1a–e). Magnified SEM images reveal that the wrinkled sheets of silica are arranged in three dimensions to form the spherical shape with a pore mouth size of 10–30 nm. The transmission electron microscopy (TEM) images indicate that the pores are radially oriented, and their sizes gradually increase from the center to the outer surface (Figure 1f–j). Interestingly, we found that the particle size of MSNs is dependent on the alkyl chain length of imidazolium bromide while the morphology and mesopore structure are not influenced by the imidazolium bromide. When the alkyl chain length of [CnMIM] Br is $n \leq 10$, the particle size is about 145 nm which is larger than the size of parent MSNs synthesized in the absence of [CnMIM] Br (Table 1 and Figure S1). However, when $n \geq 12$, the particle size of MSNs is less than that of parent MSNs. This finding is consistent with previously reported results.[45−54] The long chain amphiphilic [CnMIM] Br ILs ($n \geq 12$) can be regarded as the cosurfactant which reduces the critical micelle concentration (CMC) of cationic surfactants. As a result, the more nucleiare formed, the smaller particle sizes of MSNs are obtained.[55] Generally, the short chain ILs are often utilized as green solvent to synthesize metal or metal oxide nanoparticles. Unexpectedly, in this study, the larger size MSNs are finally produced. We believe that, probably due to the introduction of trace amount of short chain ILs, the variations of viscosity and (or) conductivity of reaction media affects the growth mode of MSNs, which resulted in the formation of larger particle size MSNs. It is well-known that ILs, particularly for 1-alkyl-3-methylimidazoliums ([CnMIM]) with short chain length can significantly decrease the viscosity of liquid systems.[56,57] This hypothesis is further proved in the following section regarding to the effect of the amount of 1-butyl-3-imidazolium bromide on the mesostructure and particle size of MSNs.

Table 1. Textural Characteristics of Calcined MSNs Synthesized in the Presence of Methylimidazolium Bromide with Different Alkyl Chain Lengths

sample[a]	S_{BET} (m^2/g)[b]	V (cm^3/g)[c]	D_{BJH} (nm)[d]	PS (nm)[e]
MSNs	460	0.88	3.3/10.6	115 ± 10
MSNs-C4	359	0.69	3.7/10.6	145 ± 15
MSNs-C8	417	0.78	3.3/10.6	145 ± 15
MSNs-C10	391	0.64	3.3/10.6	145 ± 15
MSNs-C12	448	0.79	3.3/10.6	112 ± 10
MSNs-C16	460	0.86	3.3/10.6	107 ± 10

[a]MSNs-Cn, where n represents the alkyl length of 4, 8,10,12,16, respectively. [b]Specific surface area measured from N_2 physisorption. [c]Total pore volume measured at P/P_0 = 0.99. [d]Pore diameter calculated from the BJH theoretical model. [e]Particle size distribution was determined by measuring the diameters of at least 100 particles under TEM (Figure 1). *Note that, before the nitrogen adsorption measurement, to avoid the contribution of interparticle void into the total volume and surface area, the powder of dendritic MSNs was pelleted at 10 MPa and the molar ratio of ILs to Si was fixed at 0.0095.*

The porous structure of the MSNs was further examined by N_2 adsorption–desorption measurements. All MSNs samples exhibited a type IV isotherm with a H_3 type hysteresis loop in the relative pressure range of 0.4–1.0 (Figure 2), implying the presence of various sized, slit-shaped mesopores.[27] The BJH adsorption pore volume curves, consisting of a relatively sharp

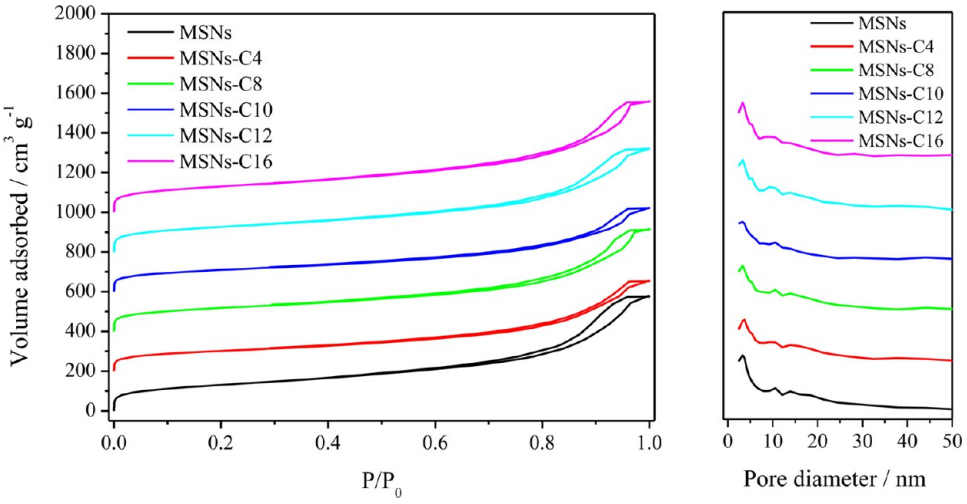

Figure 2. N_2 adsorption−desorption isotherms and pore size distribution plots of dendritic MSNs synthesized with different alkyl chain length in methylimidazolium bromide (n = 4, 8, 10, 12, 16).

peak (3 nm), a feeble shoulder peak (11 nm), and a broad peak (50 nm) (Figure 2), confirm the multimodal pore size distributions. Interestingly, all MSN samples have a uniform pore structure and very similar surface areas despite the fact that imidazolium ILs with different alkyl chain lengths were used for the preparation (Figure 2 and Table 1). This textural uniformity of MSNs particles clearly demonstrates that the variation of chain length of imidazolium ILs just affects the particle size but not the morphology and mesostructure of MSNs.

Effect of the Amount and Counteranion Type of Imidazolium ILs ([BMIM] X). The above results of alkyl chain length of imidazolium ILs on the particle size showed that the use of short-chain imidazolium ILs favors the synthesis of MSNs with larger particle size. Herein, we fixed the alkyl chain length with n = 4 and the imidazolium ILs have the same 1-butyl-3- methylimidazolium cationic moieties. The effect of amount and anionic moieties of the imidazolium [BMIM] X (X = Cl, Br, BF_4, and OTF) on the properties of dendritic MSNs were also studied. With the increase of molar ratio of [BMIM] OTF/Si from 0.000 95 to 0.028 5, the particle size of dendritic MSNs increases from 110 to 260 nm (Figure 3). However, when this ratio is further raised, the morphology and mesostructure of dendritic MSNs cannot be maintained (Figure S2), indicating that the introduction of [BMIM] OTF intervenes the interface self-assembling of cationic surfactant and silicates. Remarkably, a close examination under SEM displays that the interwrinkle distance of MSNs increased with the amount of [BMIM] OTF as shown in Figure 3c. A similar result was also reported by Lee.[26] The addition of different cosolvents such as n-butanol and 2-propanol in the reaction media alters the morphology and particle size of dendritic MSNs. The enlargement of inter wrinkle distance of MSNs with the increase of concentration of [BMIM] OTF probably led to the decreases of specific surface area and total pore volume (Figure 4 and Table 2). It is worth noting that the morphology and mesostructure of the silica, except for the particle size, are not sensitive to the type of counteranion of 1-butyl-3-methylimidazolium (Figure 5), which is consistent with the literature.[53]

In our previous report, we found that the counteranion of cationic surfactant significantly influences the morphology and

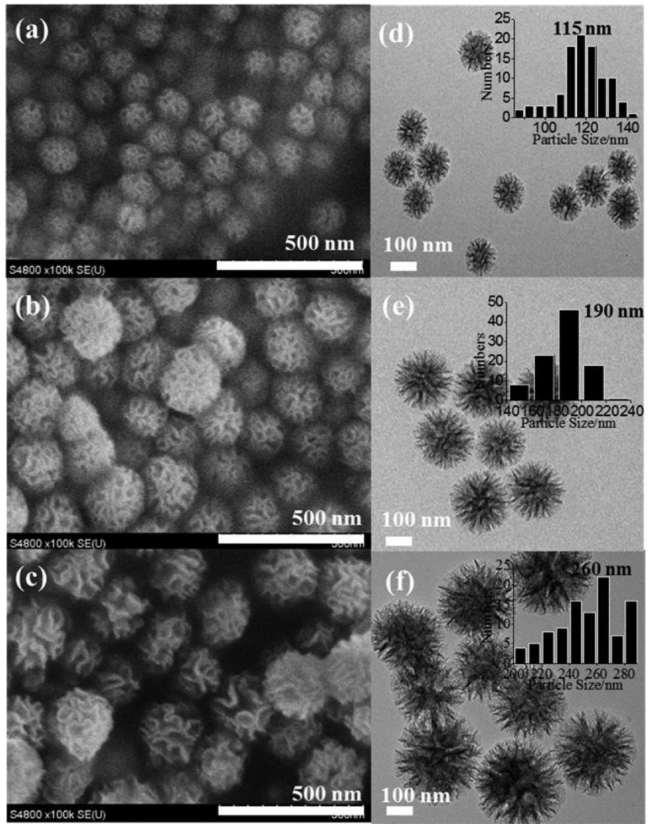

Figure 3. SEM and TEM images of dendritic MSNs synthesized with different molar ratios of [BMIM]OTF/SiO_2 (MSNs-OTF-X): X = (a and d) 0.000 95, (b and e) 0.009 5, and (c and f) 0.028 5.

mesostructure of MSNs.[27] The pivotal role of the counterions in tailoring the pore network is rationalized knowing the much lower affinity of Br^- than Tos^- for the electrical palisade of the CTA^+ micelles according to the typical anion lyotropic series order as follows: $Cl^- < Br^- < NO_3^- < I^- < SO_3C_7H_7^-$ (Tos^-).[28] Then, Tos^- competes more than Br^- against the adsorption of silicate oligomers on the micelles. This competition is at the highest at low pH. Indeed, the silanolate density (I^-) is too small to displace efficiently Tos^- anions defining typical weak templating conditions, which led to the formation of dendritic

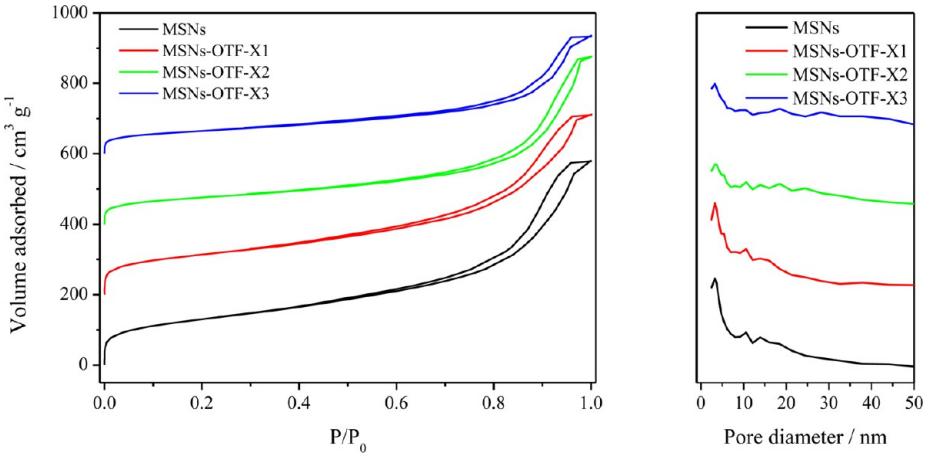

Figure 4. N_2 adsorption−desorption isotherms and pore size distribution plots of dendritic MSNs synthesized with different molar ratios of [BMIM]OTF/SiO_2 (MSNs-OTF-*X*): MSNs free of [BMIM]OTF, X1 = 0.000 95, X2 = 0.009 5, and X3 = 0.028 5.

Table 2. Textural Characteristics of Calcined Dendritic MSNs Synthesized in the Presence of [BMIM]OTF at Different Concentrations

sample[a]	S_{BET} (m^2/g)[b]	*V* (cm^3/g)[c]	D_{BJH} (nm)[d]	PS (nm)[e]
MSNs	460	0.88	3.3/10.6	115 ± 10
MSN-OTF-X1	405	0.78	3.3/10.6	115 ± 10
MSN-OTF-X2	269	0.73	3.3/10.6	190 ± 20
MSN-OTF-X3	229	0.51	3.3/10.6	265 ± 25

[a]*X* represents the molar ratio of [BMIM]OTF/SiO_2. X1, 2, and 3 represent 0.000 95, 0.009 5, and 0.028 5, respectively. [b]Specific surface area measured from N_2 physisorption. [c]Total pore volume measured at P/P_0 = 0.99. [d]Pore diameter calculated from the BJH theoretical model. [e]Particle size distribution was determined by measuring the diameters of at least 100 particles under TEM (Figure 3). *Note that, before the nitrogen adsorption measurement, to avoid the contribution of interparticle void into the total volume and surface area, the powder of dendritic MSNs was pelleted at 10 MPa.*

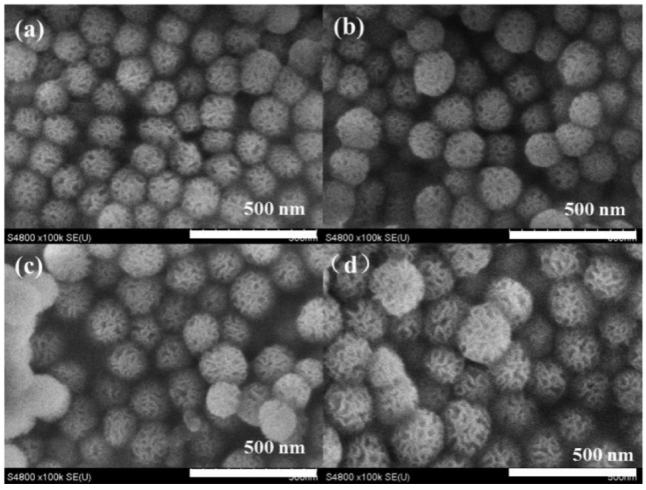

Figure 5. SEM images of dendritic MSNs synthesized using 1-butyl-3-methylimidazolium ILs with different counteranions at a fixed concentration of ILs (the molar ratio of ILS/SiO_2 = 0.0095): (a) Cl^-, (b) Br^-, (c) BF_4^-, and (d) OTF^-.

MSNs (also called stellar shaped MSNs).[27] However, in the presence of Br^-, due to the stronger interaction between silanolate group and CTA^+, the strawberry-like MSNs was formed following the conventional 2D hexagonal self-assembling process. In current research, even the ILs with different anions (X = Cl, Br, BF_4, and OTF) was added, due to the strongest affinity of TOs^- on the CTA^+, the counteranions introduced by ILs cannot interfere in the self-assembling of micelle with silicate oligomers. Thus, the morphology and mesostructure of dendritic MSNs was maintained. It is well-known that, besides of chain length of ILs, the type of counteranions also influences greatly the velocity of reaction media.[56,57] It is probably that, the addition of [BMIM]OTF with low velocity accelerates the nucleation and growth of MSNs, which leads to the formation of MSNs with larger particle size (~260 nm).

In addition, the FT-IR spectrum and thermal gravimetric analysis clearly showed that 1-butyl-3- methylimidazolium ILs were not involved on the interface self-assembling interaction between surfactant and silicates since no ILs were observed in the final MSNs powders as shown in Figures S3 and S4. Thus, we can deduce that the short chain methylimidazolium ILs only play its role as solvent for tuning the synthesis of MSNs with controlled particle size as have been done in the synthesis of metal or metal oxide nanoparticles elsewhere.[33−36,47] It was found that the relationship between molecular structure and macroscopic properties depends on transport coefficients of ionic liquids based on 1-alkyl-3-methylimidazolium cations as the concentration and length of the alkyl chain increase while keeping the same anion.[58] Viscosity decreases and conductivity increases as the alkyl chain gets shorter because van der Waals interactions decrease. Obviously, the decrease of viscosity accelerates the diffusion and aggregation of silicate covered micelles, which produces fewer nuclei. As a result, the larger size MSNs are formed when a large quantity of short chain imidazolium is used. Meanwhile, the increase of conductivity of reaction medium greatly increases the growth rate of MSNs nanoparticles, which also leads to the formation of MSNs with larger size.[59−61]

Effect of Pluronic F127 Concentration. By fine-tuning the alkyl chain length and concentration of imidazolium ILs, the dendritic MSNs with size in a range of 100−300 nm were synthesized. However, the synthesis of MSNs with diameters below 100 nm remains a great challenge. Recently, several groups reported that triblock copolymers, such as Pluronic F127, was adapted to prepare MCM-41 silica nanoparticles and nanoparticles of mordenite zeolite by suppression of grain growth.[18,42] Furthermore, the presence of Pluronic F127 did not influence the topological structure of final product. In the

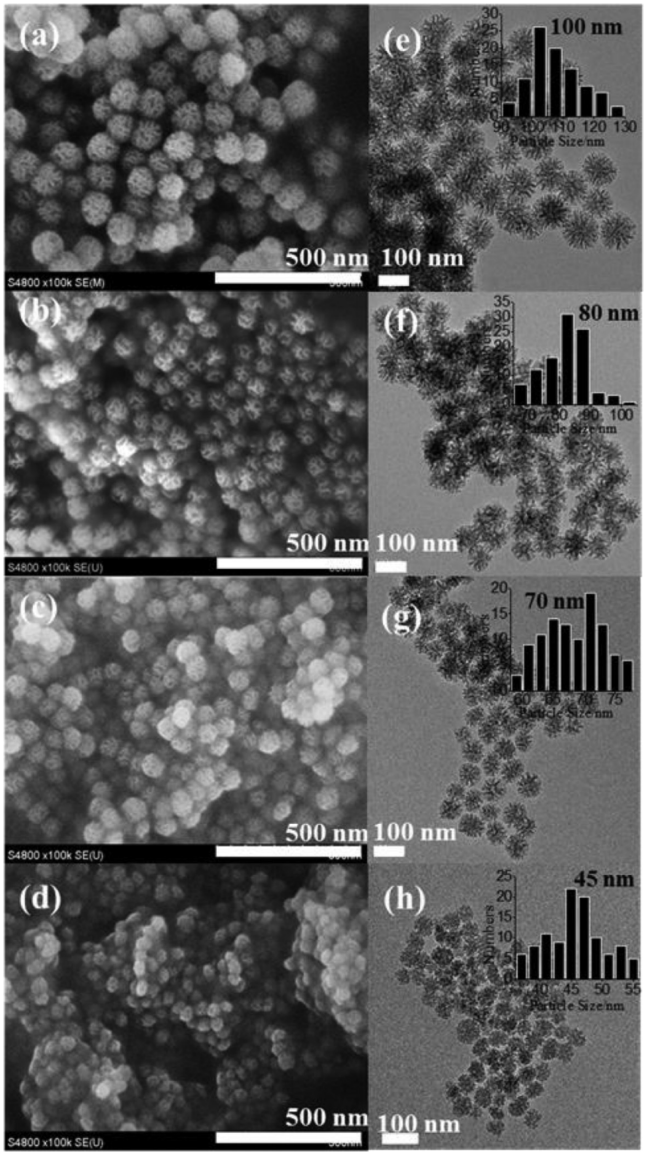

Figure 6. SEM and TEM images of dendritic MSNs synthesized using F127 as growth inhibitors with different molar ratios of F127/SiO_2 (MSNs-F127-*X*): *X* = (a and e) 0.000 48, (b and f) 0.001 6, (c and g) 0.002 4, and (d and h) 0.004 8.

light of these findings, we investigated the effect of Pluronic F127 concentration on the morphology and particle size of MSNs. Figure 6 shows SEM and TEM images of MSNs synthesized at varying concentration of F127. The control sample without F127 exhibited relatively large particles of 115 nm (Figure S1) while the coexistence of F127 dramatically reduced the size of the particles below 50 nm (≈45 nm when the molar ratio of F127/Si is 0.0048). The TEM images reveal that the pores are radially oriented, i.e., the morphology of dendritic MSNs is maintained.

The pore size distribution obtained from nitrogen adsorption−desorption isotherms (Figure 7) indicates the trimodal hierarchical porosity. The apertures of the smaller mesopores of around 3.3 nm is due to the templating effect of cetyltrimethylammonium (CTA) micelles, which indicates that the F127 molecules are not involved in the interface self-assembling interaction between silicate species and surfactants which is consistent with the reported results.[18] The larger mesopores of about 11 nm are ascribed to the radially oriented mesopores. It is worth noting that the pore size distribution centered at around 30 nm attributed to the interparticle spaces among the nanoparticles can be more easily distinguished, compared to that of dendritic MSNs prepared at high concentration of 1-butyl-3-methylimidazolium ILs (Figure 7). The textural properties of dendritic MSNs are listed in Table 3. The presence of F127

Table 3. Textural Characteristics of Calcined Dendritic MSNs in the Presence of F127 at Different Concentrations

sample[a]	S_{BET} (m^2/g)[b]	V (cm^3/g)[c]	D_{BJH} (nm)[d]	PS (nm)[e]
MSNs	460	0.88	3.3/10.6	115 ± 10
MSNs-F127-X1	385	0.85	3.3/10.6	102 ± 10
MSNs-F127-X2	380	0.95	3.3/10.6	85 ± 8
MSNs-F127-X3	380	0.89	3.3/10.6	70 ± 5
MSNs-F127-X4	372	0.77	3.3/10.6	40 ± 5

[a]*X* represents the molar ratio of F127 to Si. X1, 2, 3, and 4 represent 0.000 48, 0.001 6, 0.002 4, and 0.004 8, respectively. [b]Specific surface area measured from N_2 physisorption. [c]Total pore volume measured at P/P_0 = 0.99. [d]Pore diameter calculated from the BJH theoretical model. [e]Particle size distribution was determined by measuring the diameters of at least 100 particles under TEM (Figure 6). *Note that, before the nitrogen adsorption measurement, to avoid the contribution of interparticle void into the total volume and surface area, the powder of dendritic MSNs was pelleted at 10 MPa.*

micelles covering the MSNs suppressed the grain growth and stabilized the radially oriented mesostructures. This conclusion was further evidenced by TG analysis (Figure 8) which showed a new peak at 270 °C that can be assigned to the decomposition of F127. Remarkably, we found that the decomposition peaks of CTA^+ surfactants shifted to low temperature which implies that the obtained dendritic MSNs have much smaller particle size compared to the MSNs synthesized in the absence of F127. Also FT-IR spectrum in Figure S5 showed absorption band centered 1100 cm^{-1} assigned to stretching vibration of C−O bond of F127.We have successfully synthesized the dendritic MSNs in isolated nanograins with a diameter below 50 nm with a simple double surfactant system.

Mechanistic Insights on the Synthesis of Dendritic MSNs with Controllable Particle Size. We tentatively elucidate the effect of alkyl chain length and concentration of imidazolium ILs and concentration of F127 on both formations of CTA^+/imidazolium ILs and CTA^+/F127 aggregations in solutions and corresponding porous materials. The formation of radially oriented channel morphology may suggest a kinetically driven growth by percolation on aggregated micelles. A self-assembly of partially silicated micelles as depicted in Scheme 1 is more likely to occur with respect to the surfactant concentration that is below the surfactant CMC.[27] In the presence of imidazolium ILs, when the alkyl chain length of ILs is larger than 10, the imidazolium ILs are incorporated into the micelles of CTA^+ surfactants as a cosurfactant. The decrease of CMC of surfactant produces more micelles, thus more nuclei are formed, which leads to the dendritic MSNs with smaller size. However, when the ILs with short chain length ($n \leq 10$) are utilized as solvent, due to the decrease of viscosity and increase of conductivity of reaction media, a diffusion-limited aggregation (DLA) mostly leads to the formation of MSNs with larger particle size, similar to the growth of zeolite via a block-by-block aggregation.[62] Differing from ILs, the nonionic surfactant F127 plays a role as aninhibitor of the nanoparticle growth.

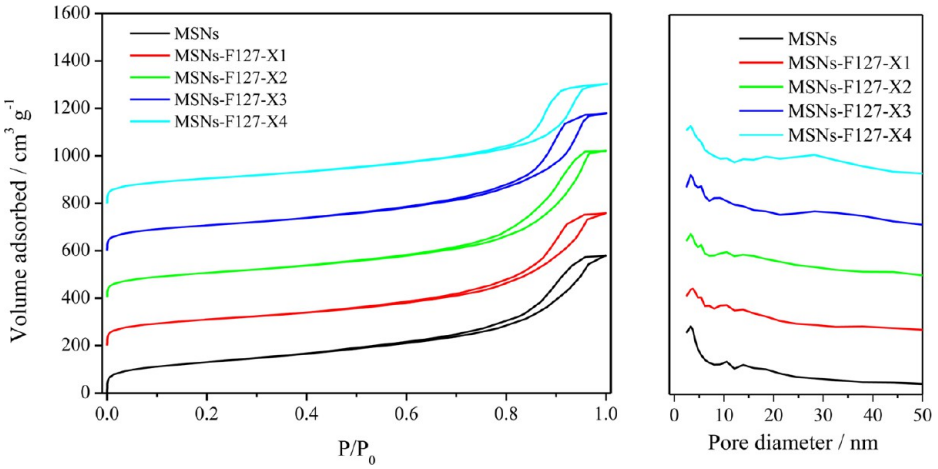

Figure 7. N_2 adsorption−desorption isotherms and pore size distribution plots of dendritic MSNs with different molar ratios of F127/SiO_2 (MSNs-F127-*X*): MSNs free of F127, X1 = 0.000 48, X2 = 0.001 6, X3 = 0.002 4, and X4 = 0.004 8.

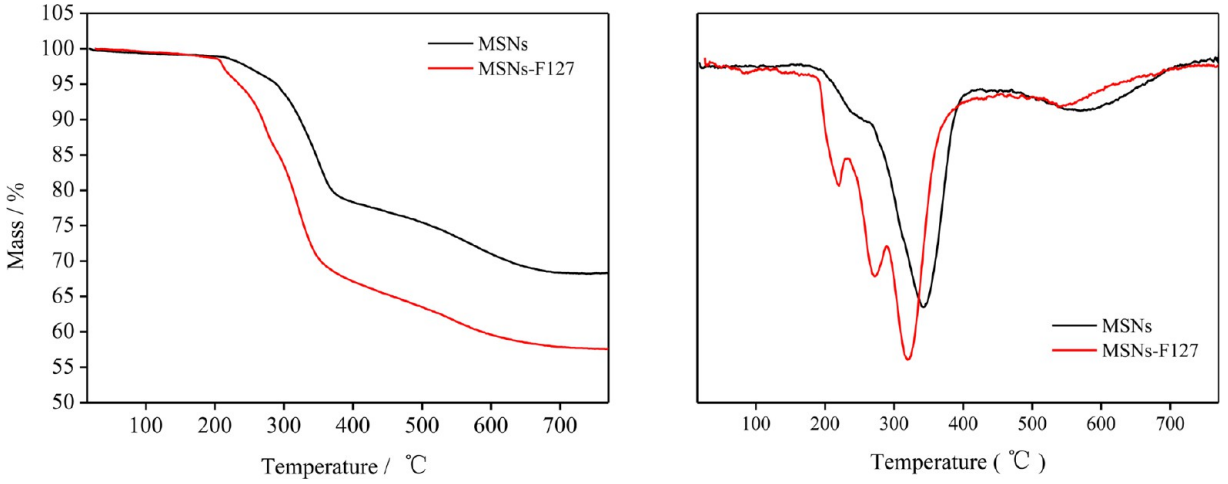

Figure 8. Thermogravimetric analysis (TG) and differential thermal gravity (DTG) of dendritic MSNs with and without F127.

Scheme 1. Mechanism of the Synthesis of Dendritic MSNs with Controllable Particle Size

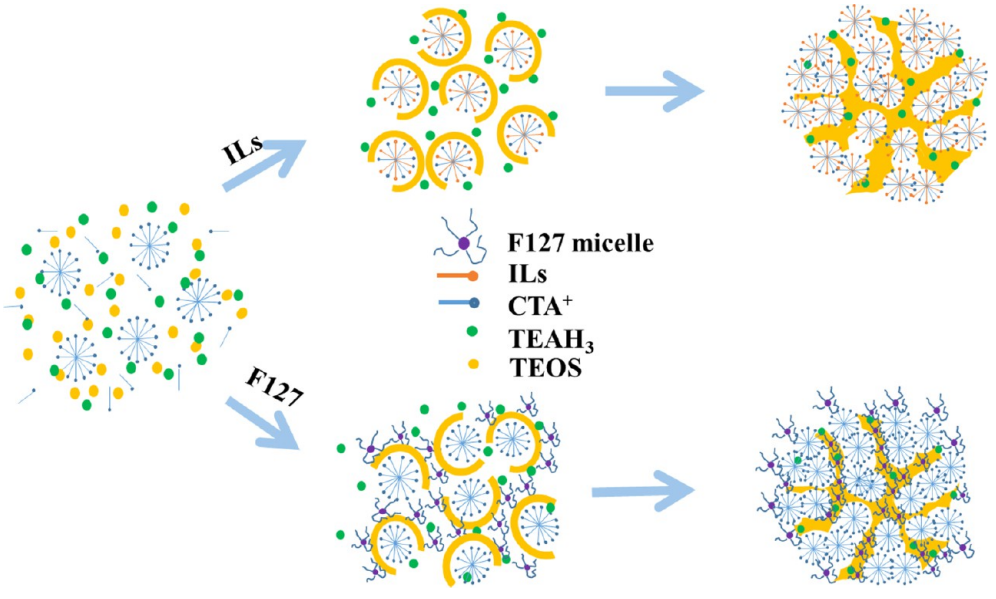

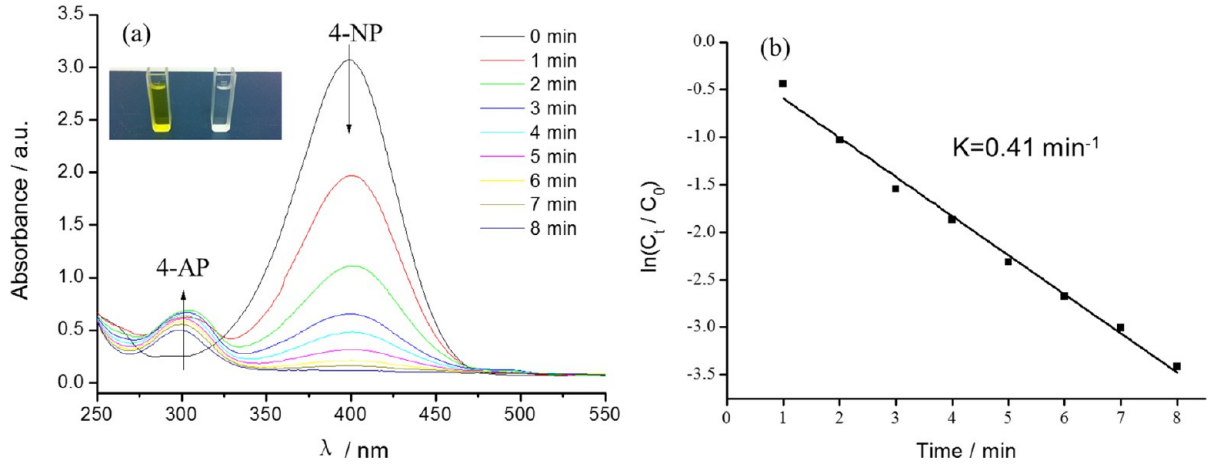

Figure 9. Successive UV−vis spectra for the reduction of 4-NP by $NaBH_4$ with Au@MSNs (a) and kinetic curves for the reduction of 4-NP (b).

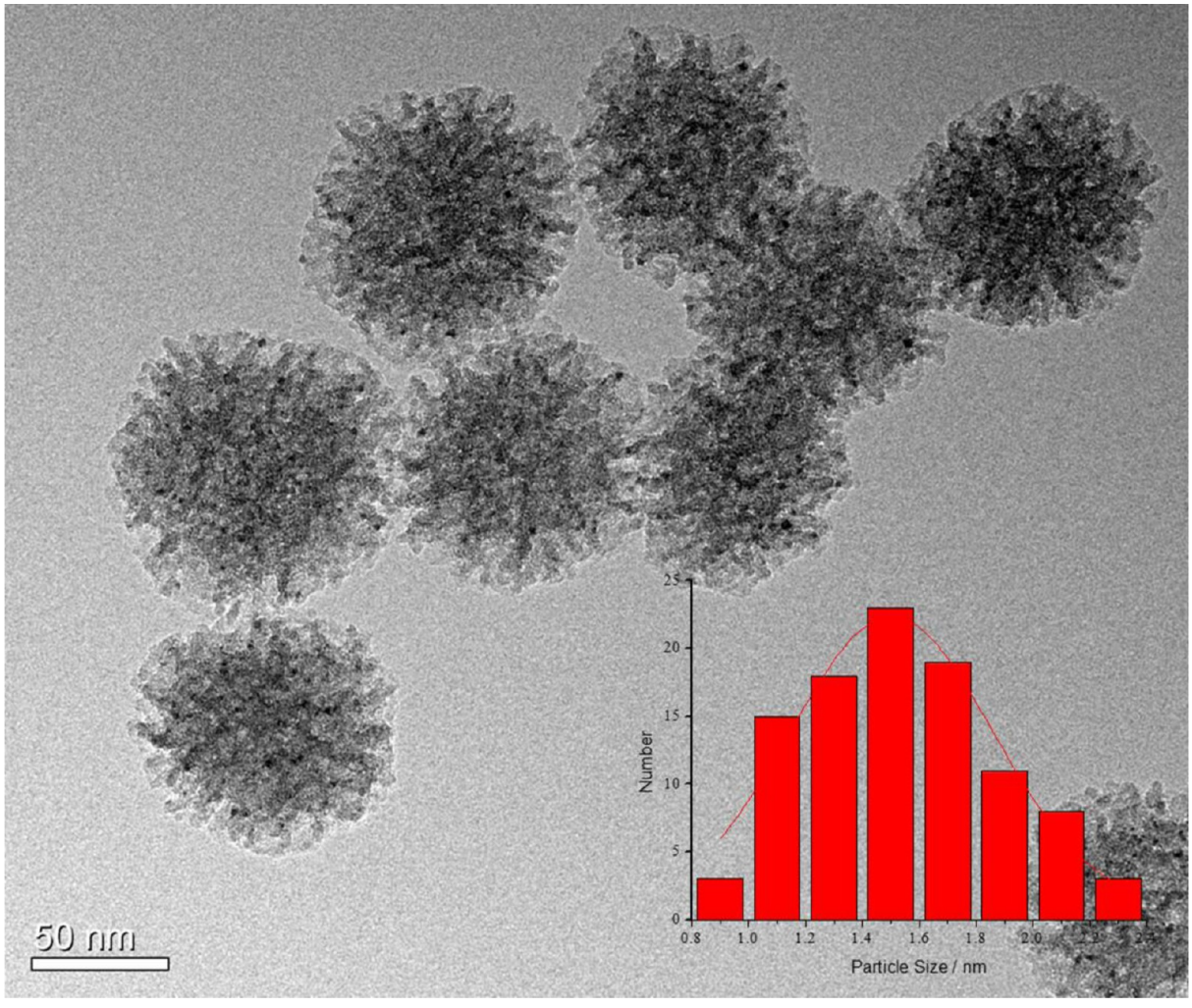

Figure 10. TEM images of Au@MSN and the size distribution of Au nanoparticles.

Because the polarity decreased with the assembly of the anionic and cationic species, the F127 could surround the ill-ordered silica-CTA^+ composites with a certain size due to a weak interaction between ionic and nonionic hydrophilic groups (Scheme 1). Therefore, the presence of F127 micelles made the nanoparticles surface covered with polymer species that suppressed the particle growth. Eventually the dendritic MSNs with smaller size less than 50 nm were obtained readily. Comparing with the conventional MCM-41 silicas, the dendritic MSNs display much smaller surface area (~450 m^2/g). It should be mentioned that, in the high pH, because of strong interaction between silicate oligomers and CTA^+, the large quantity of surface area is contributed by the surface open micropores imprinted by quaternary ammonium surfactants

heads. In contrast, the contribution of open micropores on the surface area of dendritic MSNs is dramatically diminished due to the weak templating conditions. The difference of surface area between MCM-41 and dendritic MSNs further evidence that the dendritic MSN was formed by the weak self-assembling interaction between silica and cationic surfactant, instead of classical synergetic self-assembling formation mechanism.

Liquid-Phase Reduction of 4-Nitrophenol by Au@MSNs Catalysts. The catalytic performance of the Au@MSNs was investigated by using the liquid-phase reduction of 4-nitrophenol (4-NP) by $NaBH_4$ to 4-aminophenol (4-AP) as a model reaction. Initially, the solution of 4-NP and $NaBH_4$ was yellow with the absorption peak at 400 nm recorded by UV−vis. When the catalyst of MSNs-Au was introduced into the solution, the reduction of 4-NP started immediately implied by the decreasing of absorption peak at 400 nm and the increasing of absorption peak at 300 nm. (Figure 9a). With the increasing of reaction time, the color of the reaction solution turned lighter and, finally, is colorless. The linear relationship between $\ln(C_t/C_0)$ and reaction time of the reduction reaction is demonstrated in Figure 9b, where C_t and C_0 are the concentration of 4-NP at times t and 0, which can be measured from the relative intensity of the absorbance A_t and A_0, respectively. The reduction reaction matched first-order kinetics, and the rate constant k of the reaction with the Au@MSNs catalysts was calculated to be 0.41 min^{-1}, indicating that the obtained Au@MSNs catalysts have relatively high catalytic activity.[63−67] If the reduction reaction did not start without the Au@MSNs catalysts, no obvious change of the UV−vis absorption spectra was measured. It suggests that dendritic mesostructures of the MSNs can provide convenient channels for the reactant molecules to diffuse and subsequently interact with the gold active sites with catalytic activity. TEM image in Figure 10 showed that the Au nanoparticles of size 1−2 nm were uniformly dispersed on the MSNs, which probably answers the highly catalytic performance of Au@MSNs catalysts in the liquid-phase reduction of 4-nitrophenol (4-NP) to 4-aminophenol (4-AP).

CONCLUSIONS

Dendritic mesoporous silica nanospheres with tunable particle size have been successfully synthesized by the soft-templating method using the imidazolium ionic liquids and F127 as cosurfactants. The size of resulted dendritic MSNs can be well-adjusted in a range of 50−300 nm by precise tuning of the synthesis parameters including the alkyl chain length and concentration of imidazolium and amount of F127. The different roles of ILs and F127 in the synthesis were elucidated. Using the MSNs as the silica matrix, the supported Au@MSNs catalysts showed highly catalytic performance of Au@MSNs catalysts in the liquid-phase reduction of 4-nitrophenol (4-NP) by $NaBH_4$ to 4-aminophenol (4-AP). The synthetic strategy may be used for synthesizing well-defined nanomaterials, such as metal nanoparticles, nanozeolites, and MOFs. The dendritic MSNs developed in this work are potentially important for various applications, such as drug delivery and catalysis.

ASSOCIATED CONTENT

Supporting Information

Figures S1−S5 as mentioned in the text. This material is available free of charge via the Internet at http://pubs.acs.org.

AUTHOR INFORMATION

Corresponding Author

*Tel.: +86-21-62232753. Fax: +86-21-62232753. E-mail: kzhang@chem.ecnu.edu.cn.

Notes

The authors declare no competing financial interest.

ACKNOWLEDGMENTS

This work was supported by the NSFC (21373004 and 21003050), the STCSM (10ZR1410500 and 08DZ2273300), and the Fundamental Research Funds for the Central Universities.

REFERENCES

(1) Valtchev, V.; Tosheva, L. Porous Nanosized Particles: Preparation, Properties, and Applications. *Chem. Rev.* **2013**, *113*, 6734−6760.

(2) Wu, S. H.; Mou, C. Y.; Lin, H. P. Synthesis of mesoporous silica nanoparticles. *Chem. Soc. Rev.* **2013**, *42*, 3862−3875.

(3) Argyo, C.; Weiss, V.; Bräuchle, C.; Bein, T. Multifunctional Mesoporous Silica Nanoparticles as a Universal Platform for Drug Delivery. *Chem. Mater.* **2014**, *26*, 435−451.

(4) Du, X.; Shi, B. Y.; Liang, J.; Bi, J. X.; Dai, S.; Qiao, S. Z. Developing Functionalized Dendrimer-Like Silica Nanoparticles with Hierarchical Pores as Advanced Delivery Nanocarriers. *Adv. Mater.* **2013**, *25*, 5981−5985.

(5) Lee, J. E.; Lee, N.; Kim, T.; Kim, J.; Hyeon, T. Multifunctional Mesoporous Silica Nanocomposite Nanoparticles for Theranostic Applications. *Acc. Chem. Res.* **2011**, *44*, 893−902.

(6) Slowing, I. I.; Trewyn, B. G.; Giri, S.; Lin, V. S. Y. Mesoporous Silica Nanoparticles for Drug Delivery and Biosensing Applications. *Adv. Funct. Mater.* **2007**, *17*, 1225−1236.

(7) Li, Z.; Barnes, J. C.; Bosoy, A.; Stoddart, J. F.; Zink, J. I. Mesoporous silica nanoparticles in biomedical applications. *Chem. Soc. Rev.* **2012**, *41*, 2590−2605.

(8) Vivero-Escoto, J. L.; Slowing, I. I.; Trewyn, B. G.; Lin, V. S. Y. Mesoporous Silica Nanoparticles for Intracellular Controlled Drug Delivery. *Small* **2010**, *6*, 1952−1967.

(9) Yang, P. P.; Gai, S. L.; Lin, J. Functionalized mesoporous silica materials for controlled drug delivery. *Chem. Soc. Rev.* **2012**, *41*, 3679−3698.

(10) Chen, Y.; Chen, H. R.; Shi, J. L. In Vivo Bio-Safety Evaluations and Diagnostic/Therapeutic Applications of Chemically Designed Mesoporous Silica Nanoparticles. *Adv. Mater.* **2013**, *25*, 3144−3176.

(11) Cai, Q.; Luo, Z. S.; Pang, W. Q.; Fan, Y. W.; Chen, X. H.; Cui, F. Z. Dilute Solution Routes to Various Controllable Morphologies of MCM-41 Silica with a Basic Medium. *Chem. Mater.* **2001**, *13*, 258−263.

(12) Fowler, C. E.; Khushalani, D.; Lebeau, B.; Mann, S. Nanoscale Materials with Mesostructured Interiors. *Adv. Mater.* **2001**, *13*, 649−652.

(13) Nooney, R. I.; Thirunavukkarasu, D.; Chen, Y.; Josephs, R.; Ostafin, A. E. Synthesis of Nanoscale Mesoporous Silica Spheres with Controlled Particle Size. *Chem. Mater.* **2002**, *14*, 4721−4728.

(14) Lai, C.; Trewyn, B. G.; Jeftinija, D. M.; Jeftinija, K.; Xu, S.; Jeftinija, S.; Lin, V. S. Y. A Mesoporous Silica Nanosphere-Based Carrier System with Chemically Removable CdS Nanoparticle Caps for Stimuli-Responsive Controlled Release of Neurotransmitters and Drug Molecules. *J. Am. Chem. Soc.* **2003**, *125*, 4451−4459.

(15) Möller, K.; Kobler, J.; Bein, T. Colloidal Suspensions of Nanometer-Sized Mesoporous Silica. *Adv. Funct. Mater.* **2007**, *17*, 605−612.

(16) Urata, C.; Aoyama, Y.; Tonegawa, A.; Yamauchi, Y.; Kuroda, K. Dialysis process for the removal of surfactants to form colloidal mesoporous silica nanoparticles. *Chem. Commun.* **2009**, *45*, 5094−5096.

(17) Qiao, Z. A.; Zhang, L.; Guo, M. Y.; Liu, Y. L.; Huo, Q. S. Synthesis of Mesoporous Silica Nanoparticles via Controlled Hydrolysis and Condensation of Silicon Alkoxide. *Chem. Mater.* **2009**, *21*, 3823−3829.
(18) Suzuki, K.; Ikari, K.; Imai, H. Synthesis of silica nanoparticles having a well-ordered mesostructure using a double surfactant system. *J. Am. Chem. Soc.* **2004**, *126*, 462−463.
(19) Zhang, K.; Zhang, Y.; Hou, Q. W.; Yuan, E. H.; Jiang, J. G.; Albela, B.; He, M. Y.; Bonneviot, L. Novel synthesis and molecularly scaled surface hydrophobicity control of colloidal mesoporous silica. *Microporous Mesoporous Mater.* **2011**, *143*, 401−405.
(20) Yokoi, T.; Karouji, T.; Ohta, S.; Kondo, J. N.; Tatsumi, T. Synthesis of Mesoporous Silica Nanospheres Promoted by Basic Amino Acids and their Catalytic Application. *Chem. Mater.* **2010**, *22*, 3900−3908.
(21) Polshettiwar, V.; Cha, D. Y.; Zhang, X. X.; Basset, J. M. High-Surface-Area Silica Nanospheres (KCC-1) with a Fibrous Morphology. *Angew. Chem., Int. Ed.* **2010**, *49*, 9652−9656.
(22) Nandiyanto, A. B. D.; Kim, S.; Iskandar, F.; Okuyama, K. Synthesis of spherical mesoporous silica nanoparticles with nanometer-size controllable pores and outer diameters. *Microporous Mesoporous Mater.* **2009**, *120*, 447−453.
(23) Zhang, H. J.; Li, Z. Y.; Xu, P. P.; Wu, R. F.; Jiao, Z. A facile two step synthesis of novel chrysanthemum-like mesoporous silica nanoparticles for controlled pyrene release. *Chem. Commun.* **2010**, *46*, 6783−6785.
(24) Du, X.; He, J. H. Spherical silica micro/nanomaterials with hierarchical structures: Synthesis and applications. *Nanoscale* **2011**, *3*, 3984−4002.
(25) Guo, X. H.; Deng, Y. H.; Tu, B.; Zhao, D. Y. Facile Synthesis of Hierarchically Mesoporous Silica Particles with Controllable Cavity in Their Surfaces. *Langmuir* **2010**, *26*, 702−708.
(26) Moon, D. S.; Lee, J. K. Tunable Synthesis of Hierarchical Mesoporous Silica Nanoparticles with Radial Wrinkle Structure. *Langmuir* **2012**, *28*, 12341−12347.
(27) Zhang, K.; Xu, L. L.; Jiang, J. G.; Calin, N.; Lam, K. F.; Zhang, S. J.; Wu, H. H.; Wu, G. D.; Albela, B.; Bonneviot, L. Facile Large-Scale Synthesis of Monodisperse Mesoporous Silica Nanospheres with Tunable Pore Structure. *J. Am. Chem. Soc.* **2013**, *135*, 2427−2430.
(28) Zhang, K.; Yuan, E. H.; Xu, L. L.; Xue, Q. S.; Luo, C.; Albela, B.; Bonneviot, L. Preparation of High-Quality MCM-48 Mesoporous Silica and the Mode of Action of the Template. *Eur. J. Inorg. Chem.* **2012**, *2012*, 4183−4189.
(29) Zhang, K.; Chen, H. L.; Albela, B.; Jiang, J. G.; Wang, Y. M.; He, M. Y.; Bonneviot, L. High-Temperature Synthesis and Formation Mechanism of Stable, Ordered MCM-41 Silicas by Using Surfactant Cetyltrimethylammonium Tosylate as Template. *Eur. J. Inorg. Chem.* **2011**, *2011*, 59−67.
(30) Stöber, W.; Fink, A.; Bohn, E. Controlled growth of monodisperse silica spheres in the micron size range. *J. Colloid Interface Sci.* **1968**, *26*, 62−69.
(31) LaMer, V. K.; Dinegar, R. H. Theory, Production and Mechanism of Formation of Monodispersed Hydrosols. *J. Am. Chem. Soc.* **1950**, *72*, 4847−4854.
(32) Deshmukh, R. R.; Rajagopal, R.; Srinivasan, K. V. Ultrasound promoted C-C bond formation: Heck reaction at ambient conditions in room temperature ionic liquids. *Chem. Commun.* **2001**, 1544−1545.
(33) Endres, F.; El Abedin, S. Z. Electrodeposition of stable and narrowly dispersed germanium nanoclusters from an ionic liquid. *Chem. Commun.* **2002**, 892−893.
(34) Zhou, Y.; Antonietti, M. Synthesis of Very Small TiO_2 Nanocrystals in a Room-Temperature Ionic Liquid and Their Self-Assembly toward Mesoporous Spherical Aggregates. *J. Am. Chem. Soc.* **2003**, *125*, 14960−14961.
(35) Dupont, J.; Fonseca, G. S.; Umpierre, A. P.; Fichtner, P. F. P.; Teixeira, S. R. Transition-Metal Nanoparticles in Imidazolium Ionic Liquids: Recycable Catalysts for Biphasic Hydrogenation Reactions. *J. Am. Chem. Soc.* **2002**, *124*, 4228−4229.
(36) Liu, J.; Qiao, S. Z.; Liu, H.; Chen, J.; Orpe, A.; Zhao, D. Y.; Lu, G. Q. M. Extension of The Stöber Method to the Preparation of Monodisperse Resorcinol−Formaldehyde Resin Polymer and Carbon Spheres. *Angew. Chem., Int. Ed.* **2011**, *50*, 5947−5951.
(37) Lu, A. H.; Hao, G. P.; Sun, Q. Can Carbon Spheres Be Created through the Stöber Method? *Angew. Chem., Int., Ed.* **2011**, *50*, 9023−9025.
(38) Liu, J.; Yang, T. Y.; Wang, D. W.; Lu, G. Q. M.; Zhao, D. Y.; Qiao, S. Z. A facile soft-template synthesis of mesoporous polymeric and carbonaceous nanospheres. *Nat. Commun.* **2013**, *4*, 2798.
(39) Fang, Y.; Gu, D.; Zou, Y.; Wu, Z. X.; Li, F. Y.; Che, R. C.; Deng, Y. H.; Tu, B.; Zhao, D. Y. A Low-Concentration Hydrothermal Synthesis of Biocompatible Ordered Mesoporous Carbon Nanospheres with Tunable and Uniform Size. *Angew. Chem., Int. Ed.* **2010**, *49*, 7987−7991.
(40) Tago, T.; Aoki, D.; Iwakai, K.; Masuda, T. Preparation for Size-Controlled MOR Zeolite Nanocrystal Using Water/Surfactant/Organic Solvent. *Top. Catal.* **2009**, *52*, 865−871.
(41) Ma, Z.; Yu, J. H.; Dai, S. Preparation of Inorganic Materials Using Ionic Liquids. *Adv. Mater.* **2010**, *22*, 261−285.
(42) Morris, R. E. Ionothermal synthesis-ionic liquids as functional solvents in the preparation of crystalline materials. *Chem. Commun.* **2009**, 2990−2998.
(43) Parnham, E. R.; Morris, R. E. Ionothermal Synthesis of Zeolites, Metal−Organic Frameworks, and Inorganic−Organic Hybrids. *Acc. Chem. Res.* **2007**, *40*, 1005−1013.
(44) Huddleston, J. G.; Visser, A. E.; Reichert, W. M.; Willauer, H. D.; Broker, G. A.; Rogers, R. D. Characterization and comparison of hydrophilic and hydrophobic room temperature ionic liquids incorporating the imidazolium cation. *Green Chem.* **2001**, *3*, 156−164.
(45) Fletcher, K. A.; Pandey, S. Surfactant Aggregation within Room-Temperature Ionic Liquid 1-Ethyl-3-methylimidazolium Bis-(trifluoromethylsulfonyl)imide. *Langmuir* **2004**, *20*, 33−36.
(46) Binnemans, K. Ionic liquid crystals. *Chem. Rev.* **2005**, *105*, 4148−4204.
(47) Rao, K. S.; Singh, T.; Kumar, A. Aqueous-Mixed Ionic Liquid System: Phase Transitions and Synthesis of Gold Nanocrystals. *Langmuir* **2011**, *27*, 9261−9269.
(48) Yuan, J.; Bai, X. T.; Zhao, M. W.; Zheng, L. Q. C12mimBr Ionic Liquid/SDS Vesicle Formation and Use As Template for the Synthesis of Hollow Silica Spheres. *Langmuir* **2010**, *26*, 11726−11731.
(49) Debnath, S.; Das, D.; Dutta, S.; Das, P. K. Imidazolium Bromide-Based Ionic Liquid Assisted Improved Activity of Trypsin in Cationic Reverse Micelles. *Langmuir* **2010**, *26*, 4080−4086.
(50) Rai, R.; Baker, G. A.; Behera, K.; Mohanty, P.; Kurur, N. D.; Pandey, S. Ionic Liquid-Induced Unprecedented Size Enhancement of Aggregates within Aqueous Sodium Dodecylbenzene Sulfonate. *Langmuir* **2010**, *26*, 17821−17826.
(51) Hu, J.; Gao, F.; Shang, Y. Z.; Peng, C J.; Liu, H. L.; Hu, Y. One-step synthesis of micro/mesoporous material templated by CTAB and imidazole ionic liquid in aqueous solution. *Microporous Mesoporous Mater.* **2011**, *142*, 268−275.
(52) Li, N.; Gao, Y. A.; Zheng, L. Q.; Zhang, J.; Yu, L.; Li, X. W. Studies on the Micropolarities of bmimBF4/TX-100/Toluene Ionic Liquid Microemulsions and Their Behaviors Characterized by UV−Visible Spectroscopy. *Langmuir* **2006**, *23*, 1091−1097.
(53) Wang, T. W.; Kaper, H.; Antonietti, M.; Smarsly, B. Templating Behavior of a Long-Chain Ionic Liquid in the Hydrothermal Synthesis of Mesoporous Silica. *Langmuir* **2006**, *23*, 1489−1495.
(54) Gao, F.; Hu, J.; Peng, C. J.; Liu, H. L.; Hu, Y. Synergic effects of imidazolium ionic liquids on P123 mixed micelles for inducing micro/mesoporous materials. *Langmuir* **2012**, *28*, 2950−2959.
(55) Yamada, H.; Urata, C.; Higashitamori, S.; Aoyama, Y.; Yamauchi, Y.; Kuroda, K. Critical Roles of Cationic Surfactants in the Preparation of Colloidal Mesostructured Silica Nanoparticles: Control of Mesostructure, Particle Size, and Dispersion. *ACS Appl. Mater. Interfaces* **2014**, 3491−3500.

(56) Ribeiro, M. C. C. High Viscosity of Imidazolium Ionic Liquids with the Hydrogen Sulfate Anion: A Raman Spectroscopy Study. *J. Phys. Chem. B* **2012**, *116*, 7281−7290.
(57) Singh, T.; Kumar, A. Thermodynamics of dilute aqueous solutions of imidazolium based ionic liquids. *J. Chem. Thermodyn.* **2011**, *43*, 958−965.
(58) Tokuda, H.; Hayamizu, K.; Ishii, K.; Susan, M. A. B. H.; Watanabe, M. Physicochemical Properties and Structures of Room Temperature Ionic Liquids. 2. Variation of Alkyl Chain Length in Imidazolium Cation. *J. Phys. Chem. B* **2005**, *109*, 6103−6110.
(59) Bogush, G. H.; Zukoski, C. F., IV Studies of the kinetics of the precipitation of uniform silica particles through the hydrolysis and condensation of silicon alkoxides. *J. Colloid Interface Sci.* **1991**, *142*, 1−18.
(60) Matsoukas, T.; Gulari, E. Monomer-addition growth with a slow initiation step: A growth model for silica particles from alkoxides. *J. Colloid Interface Sci.* **1989**, *132*, 13−21.
(61) Van Blaaderen, A.; Van Geest, J.; Vrij, A. Monodisperse colloidal silica spheres from tetraalkoxysilanes: Particle formation and growth mechanism. *J. Colloid Interface Sci.* **1992**, *154*, 481−501.
(62) Gao, F.; Sougrat, R.; Albela, B.; Bonneviot, L. Nanoblock Aggregation−Disaggregation of Zeolite Nanoparticles: Temperature Control on Crystallinity. *J. Phys. Chem. C* **2011**, *115*, 7285−7291.
(63) Wu, S. H.; Tseng, C. T.; Lin, Y. S.; Lin, C. H.; Hung, Y.; Mou, C. Y. Catalytic nano-rattle of Au@hollow silica: towards a poison-resistant nanocatalyst. *J. Mater. Chem.* **2011**, *21*, 789−794.
(64) Tan, L. F.; Chen, D.; Liu, H. Y.; Tang, F. Q. A Silica Nanorattle with a Mesoporous Shell: An Ideal Nanoreactor for the Preparation of Tunable Gold Cores. *Adv. Mater.* **2010**, *22*, 4885−4889.
(65) Jin, Z.; Wang, F.; Wang, J. X.; Yu, J. C.; Wang, J. F. Metal Nanocrystal-Embedded Hollow Mesoporous TiO_2 and ZrO_2 Microspheres Prepared with Polystyrene Nanospheres as Carriers and Templates. *Adv. Funct. Mater.* **2013**, *23*, 2137−2144.
(66) Wang, H.; Wang, J. G.; Zhou, H. J.; Liu, Y. P.; Sun, P. C.; Chen, T. H. Facile fabrication of noble metal nanoparticles encapsulated in hollow silicawith radially oriented mesopores multiple roles of the *N*-lauroylsarcosine sodium surfactant. *Chem. Commun.* **2011**, *47*, 7680−7682.
(67) Chen, J. C.; Xue, Z. T.; Feng, S. S.; Tu, B.; Zhao, D. Y. Synthesis of mesoporous silica hollow nanospheres with multiple gold cores and catalytic activity. *J. Colloid Interface Sci.* **2014**, *429*, 62−67.